# Agitation-free multiphoton microscopy of oblique planes

**Christopher W. Smith, Edward J. Botcherby, Martin J. Booth, Rimas Juškaitis, and Tony Wilson***

*Department of Engineering Science, University of Oxford, Parks Road, Oxford, OX1 3PJ, UK*
**Corresponding author: tony.wilson@eng.ox.ac.uk*

Received September 24, 2010; accepted October 28, 2010;
posted January 31, 2011 (Doc. ID 135626); published February 23, 2011

The scanning two-photon fluorescence microscope produces optically sectioned images from the focal plane. It is sometimes desirable to acquire images from other planes of the specimen that are inclined with respect to the focal plane. In this Letter, we discuss the issues concerned with acquiring such images together with the effects of the inclination angle on image resolution and sectioning strength. To obtain images from oblique planes at high speed, a two-photon system was built wherein a novel optical system is used to provide aberration-free scanning. © 2011 Optical Society of America

*OCIS codes:* 180.5810, 180.6900.

The scanning two-photon microscope is widely used in many areas of biological research because of its ability to provide highly resolved, optically sectioned images of thick specimens. The slice that is imaged efficiently lies close to the focal $x$–$y$ plane, and by acquiring images with different focal $z$ settings, it is possible to build three-dimensional (3D) datasets from which volumetric reconstructions can be used to study the 3D structure of the specimen in fine detail.

A long-standing problem in two-photon microscopy, and indeed microscopy in general, is that usually only the $x$–$y$ plane can be imaged at high speed and biological features of interest are seldom fortuitously aligned in this plane. For example, Bub *et al.* [1] encountered problems when imaging cardiac myocytes *in vivo*, as the cells were often found to be aligned with significant but unknown out-of-plane components. Further challenges are also apparent during live-cell imaging or *in vivo* studies when specimens exhibit time-varying behavior, as traditional $x$–$y$–$z$ image stacks can take up to a minute to acquire, so movements during this time can make the resulting data hard to interpret.

These difficulties may be addressed if one were able to image an oblique plane of the specimen directly. If such a plane were aligned with features of interest and scanned at similar rates to the $x$–$y$ plane, the resulting images may reveal useful information about the nature of the specimen with sufficient temporal resolution to adequately resolve the underlying biological processes. Göbel and Helmchen [2] have recently imaged neurons orientated perpendicular to the brain surface by scanning in an oblique plane, which permitted functional activity from across the whole cell to be observed.

A number of issues must be considered when scanning oblique planes in two-photon microscopy. If a raster trajectory is to be followed, it is first necessary to define a pair of orthogonal basis vectors along the fast- and slow-axis directions. Göbel and Helmchen defined the fast axis to lie solely in the $x$–$y$ plane, and in this way they were able to carry out the $z$ component of the scan with a relatively slow, piezodriven objective while still being able to deliver frame rates similar to those for conventional $x$–$y$ scanning. However, for some applications, such as those where the biological specimen undergoes structural changes, it is crucial that the orientation of the basis vectors be truly arbitrary. Ideally, one would be able to select a fast scan axis that is aligned with the direction in which specimen dynamics are fastest, even if this does not lie in the $x$–$y$ plane.

Another factor to be aware of when scanning oblique planes is specimen agitation; for very sensitive applications, such as patch-clamp electrophysiology, even small disturbances that result from focusing the objective lens can be detrimental. With the focusing rates required for oblique-plane scanning at high speed, specimen agitation is increased further. It is important, therefore, that the high-speed oblique-plane scan be achieved without agitating the specimen. A recently developed remote focusing method [3,4] offers solutions to both problems. This all-optical method permits the focal spot to be scanned anywhere in three dimensions inside a specimen and so does not require the objective lens or specimen to be moved physically. As a result, the specimen is not agitated, even when imaging at high speed. Unlike other optical refocusing methods of its kind, it does not introduce aberrations that degrade image quality, and so diffraction-limited performance can be achieved at all specimen depths. With this method (described below), $z$ scanning is performed by axially translating a small plane mirror with a low inertia, which permits high scan speeds in this direction. These scan speeds relax the constraint that the $z$ direction be the slow axis, and so they allow 3D scanning of planes at any arbitrary rotation at the conventional $x$–$y$ plane frame rate.

An important consideration when scanning oblique planes in the specimen is resolution. Microscope objectives generally have a limited acceptance angle, which leads to a focal spot that is better confined in the $x$ and $y$ directions than in the $z$ direction. When imaging the $x$–$y$ plane, the resolution is determined by the lateral extent of the focal spot and is therefore the same along both the $x$ and $y$ axes in the final image. This situation changes when imaging the $x$–$z$ plane, as the resolution along the $z$ direction is determined by the axial extent of the focal spot, which is not as well confined. As a result, the resolution along $z$ is poorer than along $x$, so these images possess a nonisotropic resolution that can often be seen clearly by eye or in a Fourier transform. By extension, any image of an oblique plane must also exhibit nonisotropic resolution on the basis that the focal spot has a different confinement along the different principle axes of the plane.

 

To evaluate the range of spatial frequencies that may appear in the two-photon image of an oblique plane, we consider the image formation process in Fourier space [Figs. 1(a)–1(c)]. The 3D optical transfer function (3D OTF) of a system with limited NA only spans a finite region of support in Fourier space [Fig. 1(b)], which limits the spatial frequency components of the specimen that can be imaged with the microscope. When imaging an oblique plane rotated by angle $\theta$ about the $y$ axis, the spatial frequency spectrum of the specimen is multiplied by the 3D OTF and projected along the $r'$ direction, as defined in the figure, onto the $m'$–$n$ plane with an appropriate phase factor. The following expression defines the region of support for the 3D OTF [5]:

$$|r| = \begin{cases} 1, & 0 \le l \le 2, \\ l - \frac{1}{4}l^2, & 2 < l \le 4, \end{cases} \tag{1}$$

where $l = \sqrt{m^2 + n^2}$ and $r$ are the normalized spatial frequency coordinates along the radial and axial directions respectively, that are related to the real spatial frequency coordinates via scaling factors $[n \sin\alpha]/\lambda$ and $[4n \sin^2(\alpha/2)]/\lambda$ respectively; $n$ is the refractive index of the specimen; $\alpha$ is the acceptance angle for the objective lens; and $\lambda$ is the illumination wavelength. For any oblique plane we can carry out the projection of this 3D surface numerically to find the two-dimensional region of support for the resulting image. For geometric reasons, the cutoff frequency along $y$ is unaffected by the projection process whereas the cutoff along $x'$ diminishes at higher angles. The cutoff variation in this direction is plotted for 1.15 NA and 0.8 NA water immersion lenses for $\theta$ between 0° and 90° in Fig. 1(d).

A further interesting point to consider when imaging oblique planes is that of sectioning. When imaging the $x$–$y$ plane, the section thickness is determined by the axial extent of the focal spot, whereas for the $x$–$z$ plane, it is determined by its lateral extent, which is more confined. Images acquired from steeper planes therefore draw information from a thinner region of the specimen and achieve better sectioning. One measure of section thickness for a two-photon microscope can be gained by evaluating the following expression:

$$I(z') = \iint |h(x', y')|^4 \mathrm{d}x'\mathrm{d}y', \tag{2}$$

where $h(x', y')$ is the amplitude point spread function of the imaging objective [6] and $z'$ is in the direction perpendicular to the oblique plane. By calculating the FWHM of this expression, we can find the thickness of the specimen, $\Delta z$, that is imaged effectively. This has been done for two different water immersion objectives in Fig. 1(e). As we can see, both objective lenses have a section thickness that varies significantly over the angular range.

To demonstrate oblique-plane scanning using an all-optical remote scanning technique, we built the two-photon imaging system shown in Fig. 2. An axial scan unit [7] (ASU) was incorporated to scan the focal spot in the $z$ direction. The laser source used was a Ti:sapphire laser (Tsunami, Spectra-Physics), producing 80 MHz pulses with a central wavelength of 850 nm ($\Delta\lambda \sim 50$ nm, pulse length <100 fs). This was expanded to a plane wave with Gaussian width 5 mm and directed into the lateral scan unit (LSU), comprising two orthogonal galvanometer mirrors (VM1000+, Cambridge Technology, USA), that controlled the orientation of the wavefronts. From here, the wavefronts were imaged into the pupil of $L_1$ in the ASU using a $4f$ imaging system of two achromatic doublet lenses, with focal lengths of 120 and 160 mm to produce a magnification of 4/3. $L_1$ was an Olympus UApo/340, 40X, 0.9 NA dry objective, chosen for its favorable transmission characteristics at 850 nm. Light passing through $L_1$ was reflected off mirror M (PF03-03-P01, Thorlabs) and passed back through the lens. The emerging wavefront was then reimaged into the pupil plane of $L_2$ using a $4f$ system of achromatic doublets with focal lengths of 150 mm and 200 mm respectively, for a magnification of 4/3. The choice of this magnification is not trivial and a full explanation of this parameter is presented elsewhere [4]. All experiments were performed using an Olympus UApo/340, 40X, 1.15 NA water objective for $L_2$. A polarizing beam

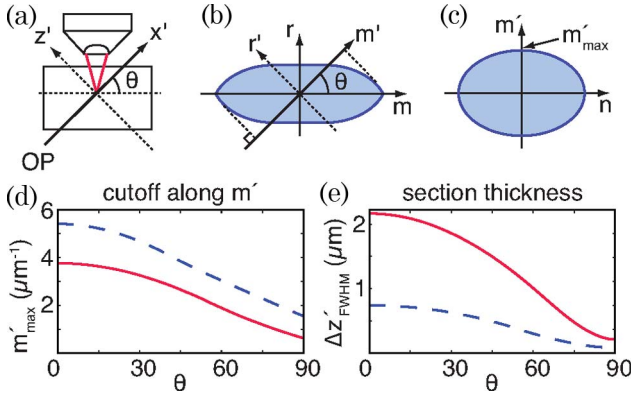


Fig. 1. (Color online) (a) Imaging oblique plane with angle $\theta$. (b) 3D OTF of the system, rotationally symmetric $r$. (c) Spatial frequency content in oblique-plane image. (Projection of 3D OTF along the $r'$ axis.) (d) and (e) Spatial frequency cutoff along inclined axis and section thickness when imaging an oblique plane for 1.15 NA (solid curve) and 0.8 NA (broken curve) water immersion lenses. $\lambda = 850$ nm.

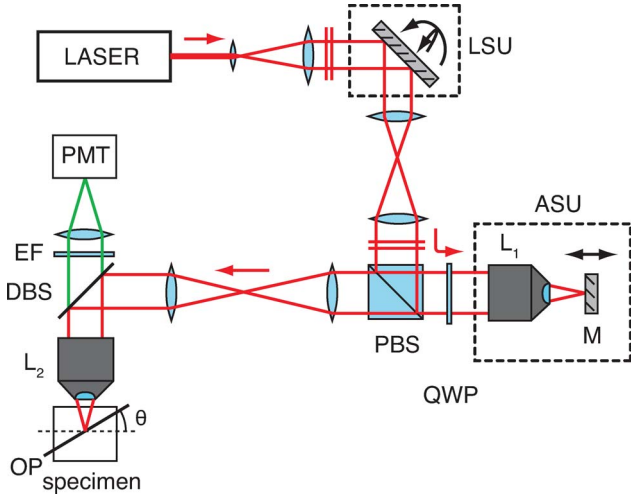


Fig. 2. (Color online) Oblique-plane scanning multiphoton microscope. The LSU scans the focal spot laterally in the specimen, and the ASU scans the spot axially. Oblique planes are scanned in three dimensions by using both the LSU and ASU.

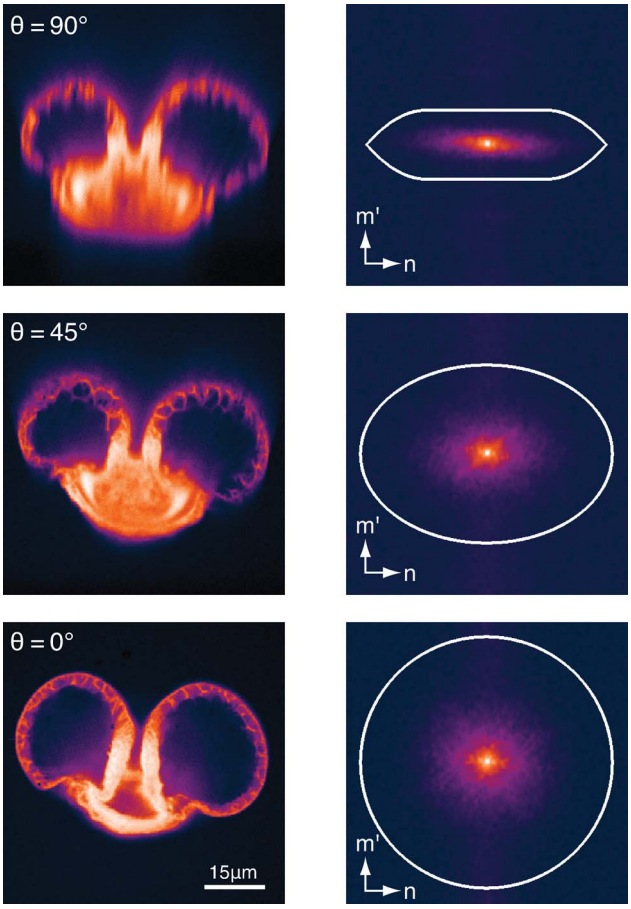


Fig. 3. (Color online) Oblique-plane images of a pollen grain with $\theta = 0°$, 45°, and 90° along with their corresponding 2D FFT plots. Calculated regions of support are marked in each case. $512 \times 512$ pixels, 10 $\mu$s per pixel.

splitter (PBS) and quarter-wave plate (QWP) ensured that all light entering the ASU was transmitted into the final stage of the system. A dichroic beamsplitter (DBS) and emission filter (EF) were used to separate fluorescence photons produced in the specimen in the range of 400–720 nm for measurement on a digital photomultiplier tube [(PMT) P30PC-54, SensTech]. Photon counting and galvanometer control were performed with a reconfigurable I/O card (PCI-7830R, National Instruments), operated from the LabVIEW environment.

We recorded a series of oblique-plane images through the center of a fluorescent pollen grain at the following angles of inclination: $\theta = 0°$, 45°, and 90°. Shown beside these in Fig. 3 are the corresponding Fourier transforms with theoretical regions of support marked for each imaging plane. We see that resolution along $n$ remains unchanged, this being the Fourier component of the rotation axis, while the resolution along $m'$ decreases as $\theta$ varies from 0° to 90°.

It is clear from these results that optical refocusing is a viable method for agitation-free high-speed oblique-plane imaging. This technique is of particular importance for *in vivo* investigations, where the plane of interest typically does not coincide with the focal plane. It has been shown that the image resolution becomes directionally dependent with increasing angle from the $x$–$y$ plane and that the sectioning thickness decreases with increasing obliquity.

A particular advantage conferred from use of the remote focusing technique is that the specimen is not agitated during the imaging process, an aspect that may be of concern if high-speed mechanical refocusing is employed. It should be noted that although detailed comments are made here in the context of two-photon imaging, the remarks apply equally to other optical sectioning instruments such as the confocal microscope, although the ASU described here would require slight modification to avoid fluorescence throughput inefficiencies on the descanning path.

C. W. Smith holds a VIP award from the Wellcome Trust, E. J. Botcherby holds an Engineering and Physical Sciences Research Council (EPSRC) postdoctoral research fellowship (EP/F042647/1), and M. J. Booth holds an EPSRC fellowship (EP/E055818/1).

## References

1. G. Bub, P. Camelliti, C. Bollensdorff, D. Stuckey, G. Picton, R. Burton, K. Clarke, and P. Kohl, Am. J. Physiol. Heart. Circ. Physiol. **298**, H1616 (2010).
2. W. Göbel and F. Helmchen, J. Neurophysiol. **98**, 3770 (2007).
3. E. Botcherby, R. Juškaitis, M. Booth, and T. Wilson, Opt. Lett. **32**, 2007 (2007).
4. E. Botcherby, R. Juškaitis, M. Booth, and T. Wilson, Opt. Commun. **281**, 880 (2008).
5. M. Gu, *Principles of Three-Dimensional Imaging in Confocal Microscopes* (World Scientific, 1996).
6. J. W. Goodman, *Introduction to Fourier Optics*, 2nd ed. (McGraw-Hill, 1996).
7. E. Botcherby, C. Smith, M. Booth, R. Juškaitis, and T. Wilson, Proc. SPIE **7569**, 756917 (2010).